



# *Origanum Elongatum* as a Green Corrosion Inhibitor for C38 Steel in an Acidic Medium

Khalil Chefira · Rachid Nmila · Tariq Benabbouha · Moustapha Siniti · Halima Rchid · Hassan El Attari

Submitted: 2 February 2021 / in revised form: 20 July 2021 / Accepted: 23 July 2021 / Published online: 7 August 2021  
© ASM International 2021

**Abstract** The extract of *Origanum elongatum* Emb. and Maire (OEE) was used as a corrosion inhibitor for C38 steel in 1N HCl medium, the inhibitory effect was studied by different techniques, weight loss and electrochemical measurements. Weight loss measurements indicate a maximum efficiency of 77.50% at a concentration of 1 g/L at 298 K. The potentiodynamic polarization shows that OEE is a mixed type of inhibitor. Electrical impedance spectroscopy measurements show an increase in charge transfer resistance accompanied by a decrease in double layer capacitance, suggesting that the OEE extract acts by adsorption on the metal surface, the decrease in the double layer is always related to the decrease in the dielectric constant and/or the increase in the thickness of the electrical double layer. Adsorption of active OEE species in 1N HCl on C38 steel follows Langmuir isotherm. A fractionation was performed on the OEE, which resulted in three different fractions. These fractions and the OEE were analysed by infrared spectroscopy, the inhibitory efficiencies of the fractions were tested by the weight loss measurements.

**Keywords** *Origanum elongatum* Emb. and Maire · Mixed inhibitor · Nyquist plot · Modified Langmuir isotherm · Physisorption · FTIR

## Introduction

Mild steel is widely used in many areas as structural material, in the automotive industry, in pipes, and in the chemical industries [1–5]. But this steel undergoes severe corrosion when pickling with hydrochloric acid and/or sulfuric acid, hence the necessity of protecting it against this phenomenon using an inhibitor in order to reduce this degradation [6–8]. It is demonstrated that molecules containing heteroatoms such as oxygen, nitrogen, sulphur, or  $\pi$ -conjugated bonds have a corrosion-proofing efficiency in an acid medium [9–11]. Several synthetic compounds have shown good corrosion inhibition, but most of them are toxic to humans and the environment [12, 13], hence the expansion in recent years of the use of plant extracts in the field of corrosion thanks to the global awareness of the protection of the environment [14–16]. These extracts do not present a great danger to the fauna and the flora and can lead to protection against corrosion quite effective [17–19]. They have advantages over chemicals because of their natural state, their low cost, their accessibility, and most importantly they are quite biodegradable. There are many studies on extracts used as corrosion inhibitors [20, 21].

According to Fennane and Rejdali [22] and Tagnaout et al [23] plants of the genus *Origanum* are widely used in the field of medicine, cosmetics and culinary uses, plants of the Lamiacea family are composed of flavonoids, tannins and polyphenols which are essentially composed of

---

K. Chefira (✉) · H. E. Attari  
Laboratoire de Chimie de Coordination et d'Analytique, Faculté des Sciences, Chouaib Doukkali, 24000 El-Jadida, Morocco  
e-mail: Khalilchefi@gmail.com

R. Nmila · H. Rchid  
Equipe de biotechnologie et valorisation des ressources végétales, Faculté des Sciences, Université Chouaib Doukkali, 24000 El-Jadida, Morocco

T. Benabbouha · M. Siniti  
Equipe de Thermodynamique, Surfaces et Catalyse, Faculté des Sciences, Université Chouaib Doukkali, 24000 El-Jadida, Morocco

aromatic rings and oxygen atoms that can adsorb to the metal surface and thus inhibit corrosion.

The *Origanum elongatum* Emb. and Maire (F/ Lamiaceae) was harvested in “Targuist” in the Rif in the north of Morocco (34°57' North 4°18' West), The composition of the essential oil of the same *Origanum* was inspected by Oualili et al [24] where they found a composition of 3 main compounds: carvacrol, para-cymene, and  $\gamma$ -terpinene.

The *O. elongatum* has been studied by some authors, A. Amakran et al studied the effect of essential oil from the aerial parts of *O. elongatum* for in vitro anti-Candida, anti-Aspergillus and anti-Rhizopus activities [25], Ramzi et al [26] conducted a study of the essential oil of *O. elongatum* on the acaricidal activity against *Varroa destructor*, In our latest work [27], we investigated the corrosion inhibitory effect of the same extract (OEE) in a 1N H<sub>2</sub>SO<sub>4</sub> medium, which showed an inhibitory efficiency of about 77.44% at a concentration of 1 g/L.

The aim of this work is to test the inhibitory capacity against corrosion extract of *O. elongatum* Emb. and Maire in HCl (1N), and this by the use of three different methods: Weight loss measurements, impedance spectroscopy and linear polarization; then a fractionation was carried out, leading to three separate fractions which were themselves tested against corrosion by the weight loss measurements.

## Experimental

### Extraction and Fractionation Method

#### Crude Extract

After harvesting, the plant (leaves and flowers) was dried at room temperature and then ground, the powder obtained was then macerated in a mixture of solvent MeOH/CHCl<sub>3</sub> (2/1, v/v) for 24 hours, the residue underwent a second maceration under the same conditions as the first, the filtrates were pooled and concentrated by evaporation of the solvents and freeze drying. The OEE was kept in a desiccator. The OEE was diluted in 1N HCl and diluted to the desired concentrations.

#### Subfractions

Thin layer chromatography was performed on the OEE extract in order to group fractions with the same chromatographic profile using a silica gel plate (pre-coated TLC plate, type SIL G 25 UV 254, size 20x20 cm), The elution was performed with three successive solvents: 1) CHCl<sub>3</sub>/MeOH/H<sub>2</sub>O (60.79/32.35/6.86; v/v/v), 2) CHCl<sub>3</sub>/MeOH/H<sub>2</sub>O (60.79/32.35/6.86; v/v/v)/ 70% EtOH (50/50; v/v), 3) 70% EtOH, the visualisation was carried out by

spraying with a mixture containing H<sub>2</sub>SO<sub>4</sub>/MeOH (50/50, v/v) followed by steaming at 110 °C for 10 min.

Three large fractions were found which were then pooled and freeze-dried.

### Weight Loss Measurements

Carbon steel specimens of the following chemical composition (wt.%) were used in the experiment: 0.38 per cent (C), 0.23 per cent (Si), 0.68 per cent (Mn), 0.01 per cent (P), 0.02 per cent (S) and the remainder iron, were used in the studies. Gravimetric method is the simplest and reliable method for the determination of inhibition efficiency. The mild steel sheets of 4cm×1cm×0.1cm were polished with a series of abrasive paper (quality 320-500-800) and cleaned with triple distilled water, leached with acetone, and then dried at room temperature. After accurate weighing, the samples were placed in a flask containing 30 ml of 1N hydrochloric acid with and without different concentrations of extract. After 6h at different temperatures, the samples were removed. To eliminate the corrosion product in an efficient way, a mechanical cleaning was carried out on the samples, based on ASTM-G1-90 (Standard Practice for Preparing, Cleaning, and Evaluation Corrosion Test Specimens), by brushing the specimens with a non-metallic bristle brush, then washed, dried, and weighed accurately using a digital balance (accuracy ± 0.1 mg), the experiments were performed three times. The average weight loss of three samples was used for the following calculations. The same procedure has been used for tests carried out at different temperatures and 1N HCl concentration and mass loss was expressed in gram and corrosion rate in g.cm<sup>-2</sup>.h<sup>-1</sup>. The corrosion rate  $C_r$  (g.cm<sup>-2</sup>.h<sup>-1</sup>) is calculated from [28]:

$$C_r = \frac{W_0 - W}{S \times t} \quad (\text{Eq 1})$$

where  $W_0$  is the initial weight before immersion, and  $W$  the final weight after the corrosion test, respectively,  $S$  is the total exposed surface of the specimens,  $t$  is exposure time. The percentage protection efficiency (%E) of extract was calculated by applying the following relation [29]:

$$\%E = \left(1 - \frac{C_r}{C_r^0}\right) \times 100 \quad (\text{Eq 2})$$

where  $C_r^0$  and  $C_r$  are the values of corrosion rate without and with inhibitor, respectively.

### Electrochemical Measurements

A three-electrode cell was used with a carbon steel (WE) working electrode, a platinum counter electrode (CE) and a saturated calomel reference electrode (SCE). The working

electrode (WE) was coated with an epoxy resin to expose a sample surface area of 1 cm<sup>2</sup>. The equipment used is EC-Lab SP200 Research Grad model/galvanostat/FRA. The data were analysed using the EC-Lab software. The polarization curves were recorded using a three-electrode system. Firstly, the working electrode is introduced into the test solution to establish the open circuit potential ( $E_{ocp}$ ) for 30 minutes. After measuring the open circuit potential, potentiodynamic polarization curves were obtained with a sweep rate of 1 mV.s<sup>-1</sup> in the potential range between ±10 V and  $E_{ocp}$ . The density of the corrosion current ( $j_{corr}$ ) was obtained by extrapolation of the anodic and cathodic Tafel to the corrosion potential. Inhibition Efficiency %E is defined as follows [30]:

$$\%E = \left(1 - \frac{j_{corr}}{j_{corr}^0}\right) \times 100 \tag{Eq 3}$$

where:  $j_{corr}$  and  $j_{corr}^0$  represent respectively the corrosion current density with and without the inhibitor.

Electrochemical impedance spectroscopy (EIS) was performed at open-circuit potential ( $E_{ocp}$ ) in a frequency range from 100 kHz to 10 mHz, with a signal amplitude perturbation of 10 mV. The inhibition efficiency %E is estimated using the following relationship [31]:

$$\%E = \left(1 - \frac{R_{corr}^0}{R_{corr}}\right) \times 100 \tag{Eq 4}$$

where:  $R_{corr}^0$  and  $R_{corr}$ , respectively represent the charge transfer resistance without and with the inhibitor.

Cyclic voltammograms (CV) were obtained by automatically changing the electrode potential from -1.2 to 1.2 V relative to the potential of the reference electrode ( $E_{ECS}$ ) at a rate of potential scanning of 50 mV.s<sup>-1</sup>.

### Fourier-Transform Infrared Spectroscopy (FTIR)

The FTIR fractions of the Crude extract and fractions were performed using a SHIMADZU FT-IR 8400S spectrometer with a Smart iTR Attachment and diamond attenuated Total Reflectance (ATR) crystal in range 500–4000 cm<sup>-1</sup>.

## Results and Discussion

### Weight Loss Studies

The values of the corrosion rate  $C_r$  (g.cm<sup>-2</sup>.h<sup>-1</sup>), the corrosion rate  $C_r$  and the efficiency of the %E inhibition obtained by the mass loss method are shown in the Table 1, where  $\theta$  is the area coverage rate [32].

Figure 1a shows the graphical representation of corrosion rate versus OEE concentration, noting that the corrosion rate decreases as the concentration of the

inhibitor is increased, however the rate decreases as the temperature increases, this is also reflected in Fig. 1b since the efficiency increases with increasing extract concentration, while it decreases with increasing temperature.

From Table 1 it is observed that this compound inhibits the corrosion of mild steel. The inhibition efficiency increases by increasing the concentration of the extract. The increase in the concentration of the extract results in an increase in the part of the metal surface covered by the inhibitory molecules and this leads to an increase in the inhibition efficiency.

Thus, these results reveal the ability of the OEE to act as a protective layer of corrosion on the mild steel and its thickness significantly affects the corrosion protection properties. It is observed that for a concentration of 1 g/L of the extract, the efficiency is about 77.50% at 298 K, compared with the work of Faustin et al [33] which tested the alkaloid extract of *Geissospermum laeve* under the same conditions as ours and which found an efficiency of 92% for a concentration of 100 mg/L at a temperature of 25 °C. The increase in temperature leads to a decrease in corrosion efficiency, which can be explained by the breakdown of physical interactions at high temperature between the adsorbed molecules of the extract and the metal surface. Generally, this type of interaction is fast but sensitive at high temperatures.

### Electrochemical Measurements

Figure 3a show the Nyquist plot of absence and presence of different concentration of OEE at room temperature, Table 2 present different parameters such as  $R_s$  (solution resistance),  $R_{ct}$  (charge transfer resistance),  $n$  (the phase shift),  $Q_{dl}$  (constant phase element) and  $C_{dl}$  (double layer capacitance), slope ( $S$ ), phase angle ( $\Phi$ ). The bode diagram was plotted for the C38 working electrode in 1 N HCl medium, in absence and in the presence of the extract at different concentrations, is shown in Fig. 3b, Table 2 presents the different parameters when it is possible to extract from the bode diagram such as slope ( $S$ ) and phase angle ( $\Phi$ ).

According to Fig. 3a, the semicircles are not perfect; this behaviour can be attributed to the frequency dispersion. For the analysis of the impedance spectra containing a capacitive loop, a simple equivalent circuit consisting of a parallel combination of a constant phase CPE element shown in Fig. 2, it is used in place of the double layer capacitance  $C_{dl}$  to represent the capacitive behaviour not conforming to the double layer [34].

This circuit makes it possible to identify the  $R_s$ , and the load ( $C_{dl}$ ) is affected by imperfections of the surface and that this effect is simulated by a constant phase element ( $Q_{dl}$ ) and the coefficient phase shift ( $n$ ), the phase shift (-

**Table 1** Corrosion parameters obtained of mild steel C38 in 1 N HCl solutions with and without addition of various concentrations of OEE

C (g/L)	$C_R$ (g.cm <sup>-2</sup> .h <sup>-1</sup> ).10 <sup>4</sup>			%E			$\theta$		
	298 K	308 K	318 K	298 K	308 K	318 K	298 K	308 K	318 K
Blank	2,34	7,29	9,77	–	–	–	–	–	–
0,1	1,02	3,46	5,60	56,21	52,60	42,73	0,5621	0,5260	0,4273
0,2	0,96	3,19	5,09	58,83	56,19	47,89	0,5883	0,5619	0,4789
0,4	0,85	2,85	4,51	63,53	60,87	53,83	0,6353	0,6087	0,5383
0,6	0,84	2,75	4,02	64,2	62,28	58,88	0,6420	0,6228	0,5888
0,8	0,63	2,34	3,86	72,99	67,93	60,46	0,7299	0,6793	0,6046
1,0	0,53	2,24	3,17	77,50	69,23	67,54	0,7750	0,6923	0,6754

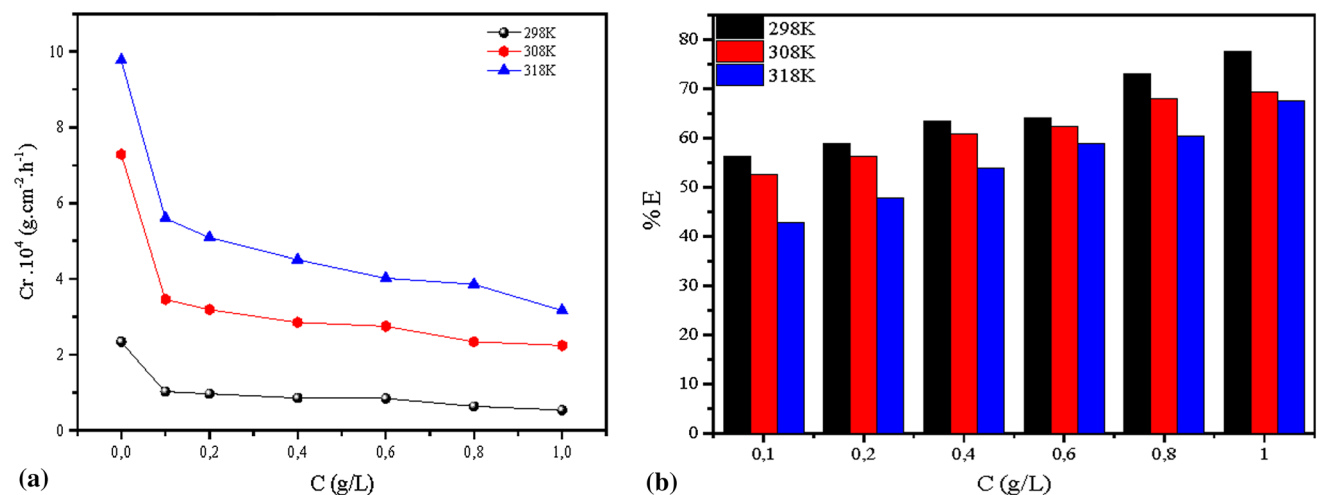


**Fig. 1** **a** Plot of corrosion rate as a function of the concentration of *O. elongatum* extract at different temperatures. **b** Inhibition efficiency as a function of OEE concentration at different temperatures

**Table 2** Electrochemical parameters deduced by EIS method (Nyquist and Bode representation) for mild steel C38 in 1 N HCl in the absence and presence of various concentrations of OEE

C (g/L)	$R_s$ ( $\Omega$ )	$Q_{dl} \cdot 10^4$ (F.s <sup>n-1</sup> )	$n$	$C_{dl} \cdot 10^4$ (F)	$R_{ct}$ ( $\Omega$ )	$-S$	$-\Phi$ (deg)	%E
Blank	1,08	7,67	0,846	3,75	25,36	0,585	49,58	–
0,1	1,13	3,19	0,883	1,84	48,52	0,739	58,19	47,73
0,2	1,81	3,75	0,865	2,03	53,19	0,719	56,70	52,32
0,4	1,66	1,53	0,861	0,72	61,39	0,712	61,25	58,69
0,6	1,06	2,20	0,874	1,20	71,01	0,783	59,99	64,29
0,8	1,40	3,17	0,868	1,79	74,70	0,740	65,56	66,05
1,0	1,89	2,24	0,895	1,46	114,40	0,788	68,94	77,83

$1 \leq n \leq 1$ ), when  $n = 0$ , the CPE represents pure resistor, if  $n = +1$ , the CPE represents pure capacitor, and if  $n = -1$ , the CPE represents inductor. To have the capacity of the double layer  $C_{dl}$ , the following formula [35]:

$$C_{dl} = Q_{dl} \times (2\pi \times f_{max})^{n-1} \tag{Eq 5}$$

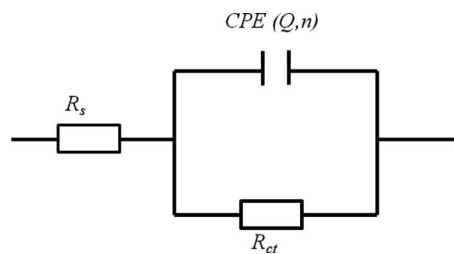


**Fig. 2** Equivalent circuit model used CPE

where  $f_{max}$  represents the frequency at which the imaginary value reaches its maximum in the representation of Nyquist,

For the calculation of the efficiency %E, Eq. 4 is used, the electrochemical parameters of  $R_{cb}$ ,  $C_{dl}$ ,  $Q_{dl}$ ,  $n$ , and  $R_s$  are calculated by the EC-Lab software and shown in Table 2, the inhibitory efficiency increases with increasing concentration of the extract in the 1 N HCl solution. The impedance data shown in Table 2 indicates that the  $R_{ct}$  and %E values increase by increasing the concentration, while the  $C_{dl}$  values decrease. The inhibition efficiency values

determined using the polarization curves are different from those determined by the EIS experiments, this difference is probably due to the shorter immersion time in the case of the polarization measurements. The decrease in  $C_{dl}$  can be explained by a decrease in the local dielectric constant and / or an increase in the thickness of the electric double layer [36]. In addition, better protection provided by an inhibitor is associated with decreased  $C_{dl}$  [37]. The adsorption of the inhibitor on the surface of the mild steel decreases its electrical capacity because it moves the molecules of water and other ions originally adsorbed on the surface [38], the decrease in this capacity with an increase in the concentration of inhibitors is often attributed to the increase in the thickness of the protective layer on the surface of the electrode this can be explained by the Helmholtz formula [39]:

$$C_{dl} = \frac{\epsilon \times \epsilon_0 \times A}{d} \quad (\text{Eq 6})$$

where  $d$  is the thickness of the protective layer,  $\epsilon$  the dielectric constant of the medium,  $\epsilon_0$  the vacuum permittivity and  $A$  is the effective surface area of the electrode.

The charge transfer resistance  $R_{ct}$  optimum's is reached at a concentration of 1 g/L which is 114.40  $\Omega$  for an efficiency of 77.83%. the increase in the value of the load transfer resistance after the increasing addition of the OEE concentration is synonymous with the formation of a protective layer on the surface of the carbon steel [40]. It can be seen that the value of  $n$  increases with respect to that of blank (0.846) by increasing the concentration of the inhibitor to an optimum value of (0.895) at a concentration of the extract 1 g/L, this can be explained as the surface of the electrode tends to behave as a perfect capacitor [41].

The linear region of the Bode representation ( $\log(f)$  vs  $\log(|Z|)$ ) should have a slope ( $-S$ ) of 1 and phase shift ( $-\Phi$ ) of  $90^\circ$  for an ideal capacitor. The experimental  $S$  values are calculated and given in Table 2, it is found that the  $-S$  values decrease compared to blank (0.585) with increasing the extract concentration for the OEE to reach a maximum value of (0.788) at a concentration of 1 g/L, it can also be seen that the phase shift ( $-\Phi$ ) increases by increasing the concentration of the inhibitor and then passes from  $49.58^\circ$  for the blank to  $68.94^\circ$  for a concentration of 1 g/L. We can deduce that our system tends to behave like a pure capacity [42].

The cyclic voltammogram of C38 in 1 N HCl solutions without and containing different concentrations of OEE was recorded and is shown in Fig. 3. The potential was initiated at  $-1200$  mV at a scan rate of  $50$  mV.s $^{-1}$ .

On this voltammogram the anodic and cathodic branches show narrow regions with no dissolution peaks, on closer inspection the anodic current region increases until the potential is reversed for all the solutions studied, the Fig. 4.

also shows that the cathodic current decreases more significantly than the anodic current as the OEE concentration increases.

Finally, it can be deduced that these results confirm the results found in the linear polarization part that the inhibitor acts as a mixed inhibitor and acts on both the anodic and cathodic reaction with a cathodic preference, and that the adsorbed species adsorb physically on the metal surface [43].

Figure 5. illustrates typical anodic and cathodic potentiodynamic polarization curves for carbon steel in 1N HCl in the absence and presence of various concentrations (from 0.1 to 1g/L) of the extract ambient temperature. The corrosion current density ( $j_{corr}$ ) was calculated from the intersection of the Tafel cathode and anode lines.

The efficiency %E was calculated from Eqm 3 and shown in Table 3, it's found that the addition of the extract implies an increase in the inhibition against corrosion which reaches a maximum value of 74.14% at 298 K at a concentration of 1 g/L of the extract.

The values of the electrochemical parameters such as corrosion potential ( $E_{corr}$ ), corrosion current density ( $j_{corr}$ ), Tafel slopes ( $\beta_c$  and  $\beta_a$ ) and inhibition efficiency %E were calculated from these curves and given in Table 3, according to Benabbouha et al [44], the  $E_{corr}$  does not vary beyond  $\pm 85$  mV this indicates that the OEE acts as a mixed inhibitor in 1 N HCl medium with a slight displacement of the cathodic side [45], and that the cathodic and anodic slopes ( $\beta_c$  and  $\beta_a$ ) for the inhibitor under study remain almost constant, which means that the mechanism of the electrode reactions is not changed [46].

In addition, the polarization curve in 1 g/L of inhibitor is characterized by the presence of an anode breakdown potential  $E_b$ , the presence of such a potential is characteristic of the formation of an anodic protective layer on the metal surface [46]32. From the Fig. 5, a clear distinction can be made between a decrease in anode and cathode currents as the OEE concentration increases, the curves obtained from the Tafel polarization studies showed that the values of  $j_{corr}$  increased from  $240.28$   $\mu\text{A}\cdot\text{cm}^{-2}$  of blank to  $62.13$   $\mu\text{A}\cdot\text{cm}^{-2}$  for a concentration of 1 g/L.

#### Adsorption Isotherms

It has been shown that the type of adsorption depends on the structure of the inhibitor molecule and/or the charge on the metal surface [47]. The use of adsorption isotherms therefore gives indications on the interactions between the inhibitor molecules but also indications on the interactions between the metal surface and these molecules, the adsorption results of our extract obey the modified Langmuir isotherm after testing several isotherms such as Frumkin, Temkin,  $\theta$  El-Awady and Freundlich [48–51];

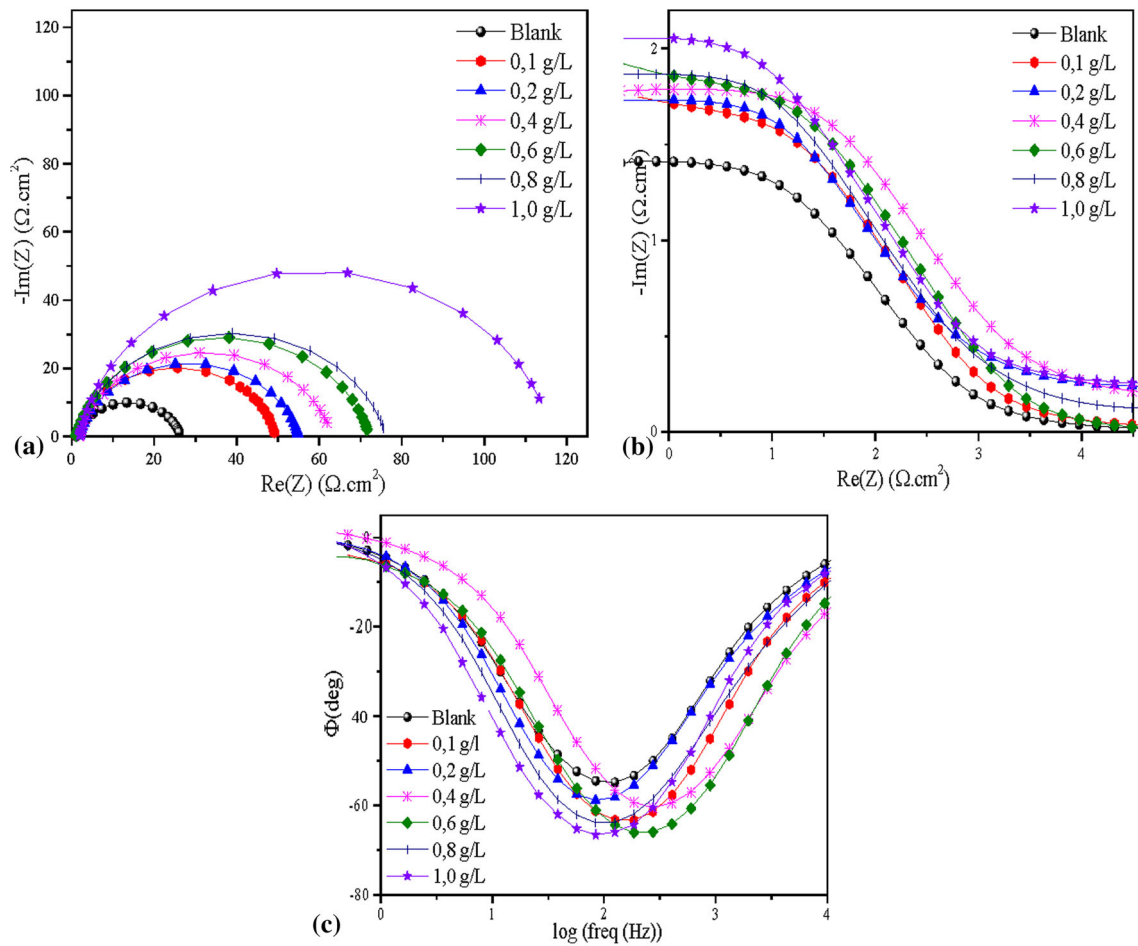


**Fig. 3** a EIS b and c bode diagrams for mild steel C38 in 1 N HCl with different concentrations of OEE at 298 K

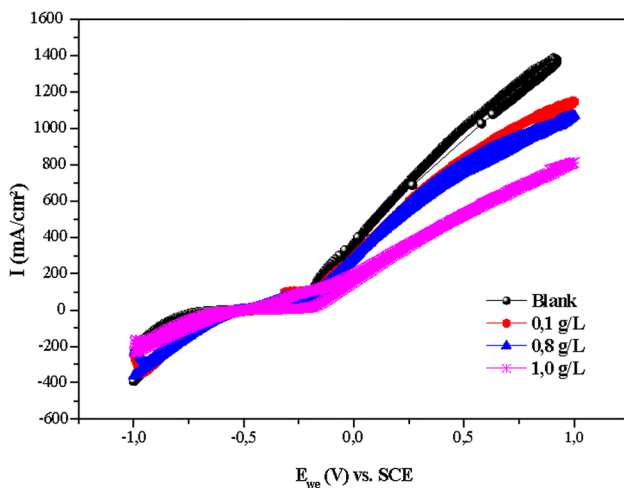


**Fig. 4** Cyclic voltammety of C38 in 1 N HCl solution free and inhibited by different concentrations of *O. elongatum* extract. Scanning rate  $50 mV \cdot s^{-1}$

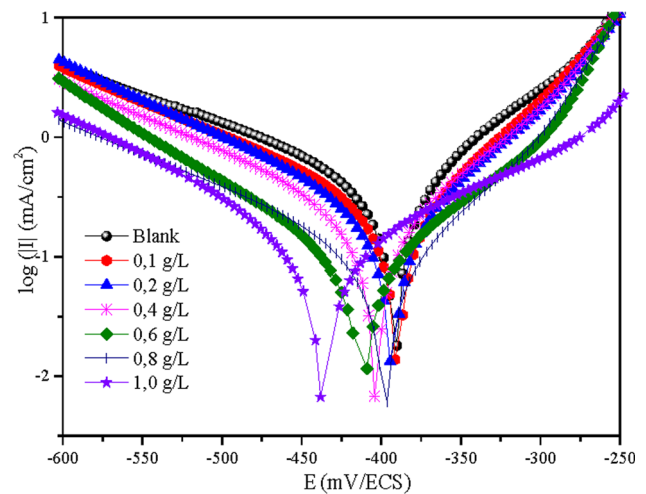


**Fig. 5** Cathodic and anodic potentiodynamic polarization curves of mild steel C38 in 1 N HCl and different concentration of extract

**Table 3** Electrochemical data from Tafel curves carried out in 1 N HCl in absence and presence of *Origanum elongatum* extract

C (g/L)	$\beta_a$ (mV.dec <sup>-1</sup> )	$\beta_c$ (mV.dec <sup>-1</sup> )	$E_{corr}$ (mV vs ESC)	$j_{corr}$ (μA.cm <sup>-2</sup> )	%E
Blank	77.4	159.0	-390.97	240.28	-
0,1	78.6	141.9	-384.33	124,25	48,29
0,2	76.9	134.6	-392.44	102,24	57,45
0,4	67.9	118.5	-402.33	92,29	61,59
0,6	99.3	121.4	-407.92	76,60	68,12
0,8	68.8	139.0	-397.10	62.13	74.14
1,0	68.2	138.4	-413.50	58.41	75.69

**Table 4** Adsorption parameters of OEE on C38 steel by different adsorption isotherms

	T(K)	R <sup>2</sup>	n	K <sub>ads</sub> (L/g)	ΔG <sub>ads</sub> (kJ/mol)
Langmuir modified	298	0,9855	1,24	12,21	-23,32
	308	0,9961	1,39	16,97	-24,94
	318	0,9896	1,41	10,09	-24,37
Frumkin	α				
	298	0,9256	3,14	0,014	-6,62
	308	0,9748	3,81	0,008	-5,18
El-Awady	I/y				
	298	0,8117	0,39	13,94	-23,64
	308	0,9456	0,30	12,12	-24,08
Freundlich	n				
	298	0,8699	0,13	0,74	-16,35
	308	0,9677	0,12	0,68	-16,72
	318	0,9794	0,19	0,65	-17,12

The values of the different parameters of the isotherms used in this study are shown in Table 4:

$$\text{Modified Langmuir : } \frac{C}{\theta} = nC + \frac{n}{K_{ads}} \tag{Eq 7}$$

$$\text{Temkin : } \theta = \frac{-2303 \log K_{ads}}{2a} - \frac{2303 \log C}{2a} \tag{Eq 8}$$

$$\text{El-Awady : } \log \left( \frac{\theta}{1-\theta} \right) = \log K + y \log C \tag{Eq 9}$$

$$\text{Freundlich : } \log \theta = \log K_{ads} + n \log C \tag{Eq 10}$$

where C is the OEE concentration used, is the metal surface coverage rate and K<sub>ads</sub> is the adsorption equilibrium constant, n in the Langmuir isotherm represents the number of active molecules adsorbed per active site on the metal surface [52], the parameter a in the Temkin isotherm gives an idea of the interaction inside the adsorbed layer [35], the value of I/y represents the number of active sites on the

metal surface that will be occupied by a single active molecule [53], n of the Freundlich isotherm describes the ease with which the active species adsorb on the surface of the metal, it is generally known that an value between 0 and 1 adsorption is easy while an n ≥ 1 adsorption is moderate or difficult [48].

The Fig. 6. shows representative graphs of the relationship between C and θ at different temperatures ranging from 298K to 318K for the five isotherms,

The parameter n of the modified Langmuir isotherm which is greater than the unit ( 1,24, 1,39 and 1,41) in our study makes it possible to say that one or more adsorbed active species occupy more than one active site [48], the positive value of Frumkin’s parameter a ( 3,14, 3,81 and 2,98) suggests that there is attraction within the layer of adsorbed molecules [54], The value lower than the unit of I/y (0,39, 0,30 and 0,41) implies that the active molecules will occupy more than one active site and this is in accordance with the interpretation of parameter n of the Langmuir isotherm [55], it can also be noted that a value of I/y less than unity suggests that a multilayer of active molecules will be adsorbed on the metal surface [56], the interaction parameter of the Freundlich isotherm n is between 0 and 1 which indicates that the adsorption of the active molecules on the metal surface is easily achieved [57].

To choose the isotherm best adapted to our study, the authors often base themselves on the correlation coefficient R<sup>2</sup> which must be as close as possible to 1, for us the modified Langmuir isotherm represents the best values of R<sup>2</sup> (0.9855, 0.9961 and 0.9896) compared to the other isotherms used in this study. Therefore the adsorption of OEE obeys the modified Langmuir isotherm [58], Table 5 represents the values of the correlation coefficient R<sup>2</sup>, the ΔH<sub>ads</sub>, ΔS<sub>ads</sub> and the free adsorption standard energy ΔG<sub>ads</sub> calculated from the following equation [57]:

$$\Delta G_{ads} = -RT \ln(C_{H_2O} \times K_{ads}) \tag{Eq 11}$$

where C<sub>H<sub>2</sub>O</sub> in g/L and K<sub>ads</sub> in L/g, the negative ΔG<sub>ads</sub> values suggest that the adsorption process of active molecules is spontaneous, if we look closely at the Table 5 we can see that ΔG<sub>ads</sub> values vary between -23.32 and -24.94 kJ/mol, and it is recognized that absolute ΔG<sub>ads</sub> values between 20 and 40 kJ/mol define a mixed adsorption process mixed between physisorption and chemisorption [59], The values ΔH<sub>ads</sub> and ΔS<sub>ads</sub> were calculated from the following equation [60]:

$$\Delta G_{ads} = \Delta H_{ads} - (T \times \Delta S_{ads}) \tag{Eq 12}$$

The negative value of ΔH<sub>ads</sub> indicates an exothermic process which is related to the two types of adsorption-physisorption and chemisorption, while an endothermic process is related to chemisorption, in our study the

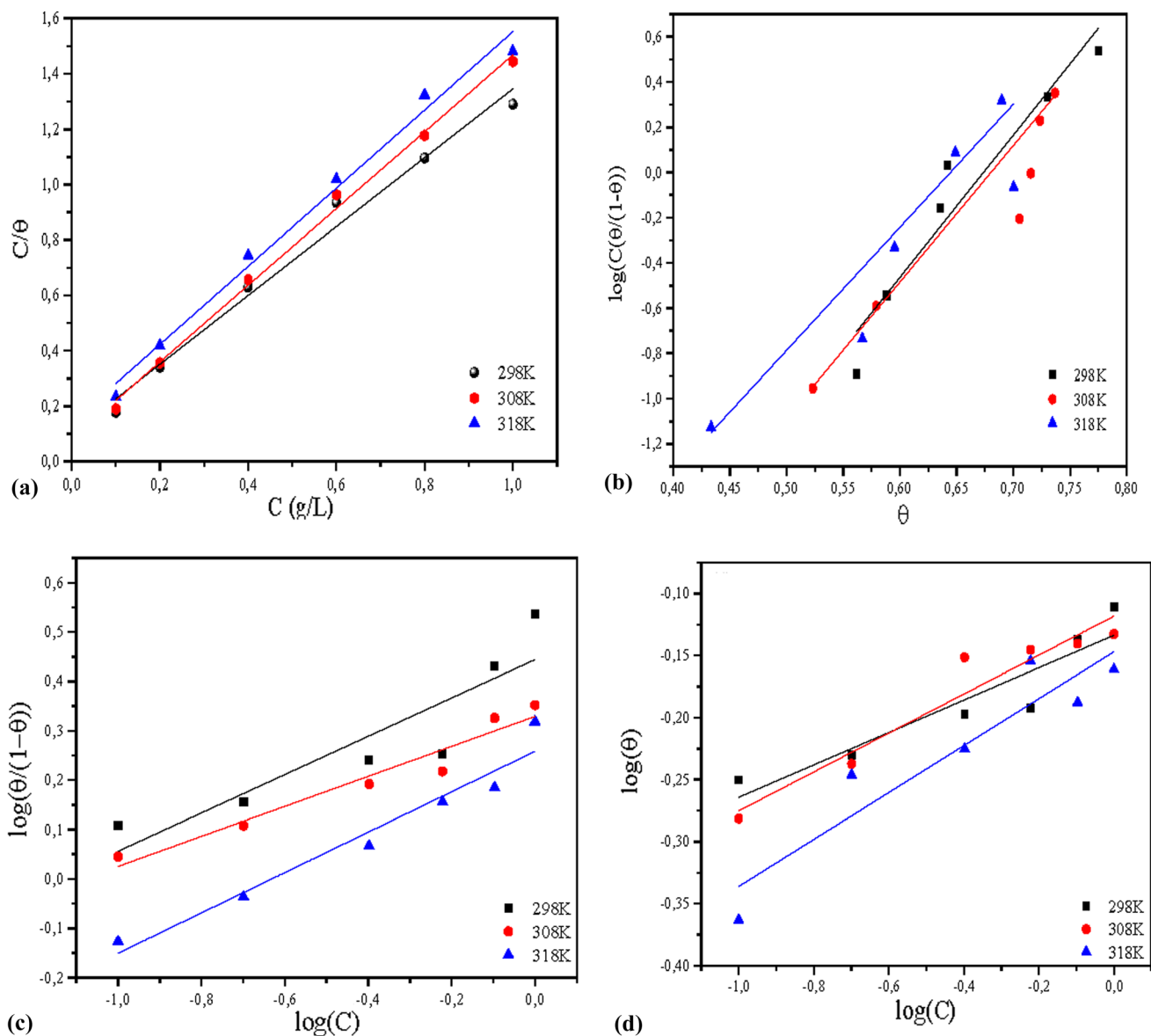


**Fig. 6** Adsorption isotherms of OEE, **a** Langmuir modified isotherm, **b** Frumkin isotherm, **c** El-Awady isotherm and **d** Freundlich isotherm

**Table 5** Adsorption thermodynamics constant and entropy energy of adsorption of the *Origanum elongatum* extract for carbon mild steel in 1 N HCl in different temperature

T (K)	$\Delta G_{ads}$ (kJ/mol)	$\Delta H_{ads}$ (kJ/mol)	$\Delta S_{ads}$ (J/mol. K)
298	-23,32	-8,04	52,5
308	-24,94		
318	-24,37		

negative value shows that we have an exothermic process, and since the absolute value of  $\Delta H_{ads}$  (8,04 kJ/mol) is less than 40kJ/mol therefore we can conclude that we have a physisorption during the adsorption of the active molecules of the OEE on the metal surface [29, 61].

The positive  $\Delta S_{ads}$  value is the result of the desorption of the water molecules adsorbed on the metal surface and their replacement by the active molecules of the OEE, resulting in an increase in the entropy of the solvent during the adsorption process [28].

#### Activation Parameters and Temperature Effect

The kinetic parameters were calculated using the following formula [62]:

$$\text{Log}(C_r) = \text{Log}(A) - \frac{E_a^*}{2303 \times R \times T} \quad (\text{Eq } 13)$$

where  $E_a^*$  is the apparent activation energy,  $R$  is the universal gas constant,  $A$  is the Arrhenius pre-exponential



constant,  $T$  is the absolute temperature, Fig. 7a shows Arrhenius plots for corrosion rate of mild steel C38, the values of  $E_a^*$  are given in Table 6.

According to Table 6, the values of  $E_a^*$  are determined by the slope of the graphs  $\log(Cr)$  vs  $1/T$ , according to the according to the Fig. 7a and Table 6, we clearly notice the increase in the value of activation energy of different solution compared to the blank, this increase is attributed to a significant decrease in the species adsorbed on the metal surface as the temperature rises. It can then be suggested that the increase in temperature has more of an effect in favouring desorption than adsorption of OEE molecules, which causes a greater surface area of the steel to come into contact with the corrosive medium, thus explaining the increase in  $C_r$  when the temperature rises [57, 25].

$$\text{Log}\left(\frac{C_r}{T}\right) = \text{Log}\left(\frac{R}{h \times N}\right) + \frac{\Delta S_a^*}{2303 \times R} - \frac{\Delta H_a^*}{2303 \times R \times T} \tag{Eq 14}$$

where  $h$  is plank's constant,  $N$  is Avogadro's number,  $\Delta S_a^*$  and  $\Delta H_a^*$  are the entropy and enthalpy of activation, respectively [63]. Figure 7b shows the plot of  $\log(Cr/T)$  vs  $1/T$ .  $\Delta H_a^*$  and  $\Delta S_a^*$  are obtained with the slope and intercept respectively. All kinetic parameters are shown in Table 6, it can be seen that  $\Delta H_a^*$  is positive which allows to say, according to Gowraraju et al [64], that the endothermic nature of the steel dissolution process, the  $\Delta S_a^*$  values of solutions containing OEE are generally more positive than those of the solution containing HCl alone, suggesting an increase in disorder when switching from reagents to activated complexes [28].

The difference between  $E_a^*$  and  $\Delta H_a^*$  remains practically unchanged, which makes it possible to verify

equation (15) between these two parameters representing the concept of the ransition states theory [65, 66].

$$E_a^* - \Delta H_a^* = R \times T \tag{Eq 15}$$

### Fractionation and Grouping of Fractions

After fractionation on a silica gel column of type G60 (70–230 mesh), to group the fractions containing the same type of molecules a thin layer chromatography with a mobile phase  $S_1$  is performed, the figure shows the different fractions and their grouping.

According to the results of the thin film separation, three large fractions were found which were then pooled and freeze-dried. Gravimetric tests were then carried out on these fractions and the results are shown in the Table 7, also Fig. 8a shows the corrosion rate of the three fractions  $H_1$ ,  $H_2$  and  $H_3$  as a function of concentration, while Fig. 8b shows the graphical representation of the efficiency of the fractions as a function of concentration.

**Table 6** Activation parameters,  $E_a^*$ ,  $\Delta H_a^*$ ,  $\Delta S_a^*$ , and Pre-exponential factor ( $A$ ), of the dissolution of C38 in 1 N HCl in the absence and presence of various concentrations of OEE

C (g/L)	A (g.cm <sup>-2</sup> .h <sup>-1</sup> ) .10 <sup>7</sup>	$\Delta H_a^*$ (kJ/mol)	$\Delta S_a^*$ (J/mol. K)	$E_a^*$ (kJ/mol)	$E_a^* - \Delta H_a^*$
Blank	0,23	54,09	-569,62	56,64	2,55
0,1	7,36	64,83	-540,64	67,39	2,56
0,2	3,97	63,46	-545,76	66,02	2,56
0,4	3,58	63,49	-546,63	66,05	2,56
0,6	7,00	59,45	-560,21	62,01	2,56
0,8	26,60	69,18	-529,94	71,75	2,57
1,0	16,80	68,36	-533,78	70,92	2,56

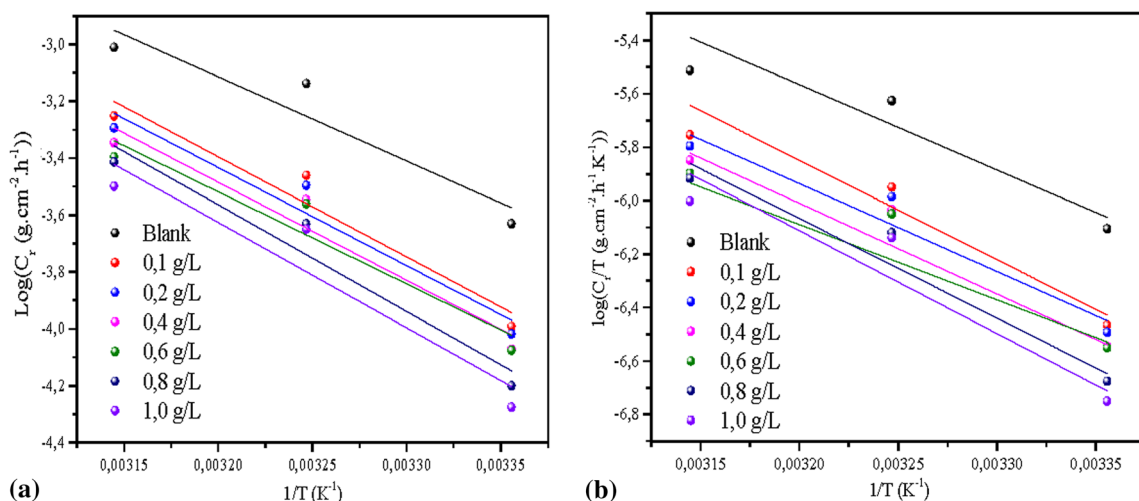


**Fig. 7** Arrhenius plots of **a**  $\log(Cr)$  versus  $1/T$ , and **b**  $\log(Cr/T)$  versus  $1/T$  in the absence and presence of different concentrations of *Origanum elongatum* extract

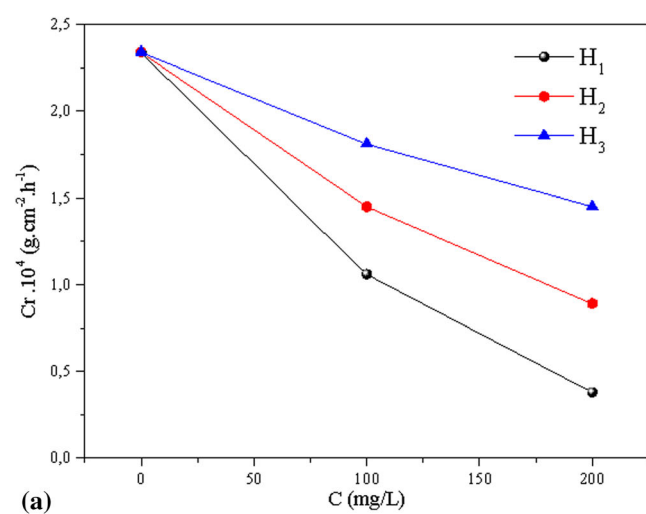
According to the Table 7, it can also be seen that the three fractions have an inhibiting effect against corrosion, which implies the existence of several active molecules containing different functions that can adsorb on the metal surface. The results of the fraction mass loss tests on C38 steel fractions in 1N HCl show that the H<sub>1</sub> fraction represents a higher inhibition efficiency followed by the second H<sub>2</sub> fraction and then the third fraction H<sub>3</sub>, based on the increasing polarity of the solutions S<sub>1</sub>, S<sub>2</sub> and S<sub>3</sub> (S<sub>1</sub>> S<sub>2</sub>> S<sub>3</sub>) it can be said that the polarity of the H<sub>1</sub>, H<sub>2</sub> and H<sub>3</sub> fractions also increases (H<sub>1</sub>>H<sub>2</sub>>H<sub>3</sub>).

### FTIR Spectroscopy

Huda Jasim Al-Tameme et al. [67] who gave the chemical composition of the methane extract of a species of *Origanum* which contains mainly alkaloids, flavonoids contain

**Table 7** Results of fractions weigh loss tests in 1N HCl at 298 K

	Blank	$C_r$ (g.cm <sup>-2</sup> .h <sup>-1</sup> ) × 10 <sup>4</sup> 2,34	%E
100 mg/L	H <sub>1</sub>	1,06	54,70
	H <sub>2</sub>	1,45	38,03
	H <sub>3</sub>	1,81	22,65
200 mg/L	H <sub>1</sub>	0,38	83,96
	H <sub>2</sub>	0,89	61,97
	H <sub>3</sub>	1,45	38,03



mostly C=O, C=C aromatic functions and OH, which are capable of acting against corrosion.

According to the IR graphs in Fig. 9, our extract is made up of different types of molecules, the most interesting are those which contain functions with which the molecules are capable of adsorbing on the metal surface (aromatic C=C, OH; or C=O...), so the study opens the door to several perspectives we are looking for the natural molecule(s) from plant matter capable of inhibiting the corrosion of C38 steel in an acidic environment.

### Proposed Adsorption Mechanism

It is recognized that the adsorption phenomenon is influenced by the nature of the metal, the corrosive environment and the nature of the inhibiting molecule(s) [36], The inhibitor molecule(s) may also adsorb to the steel surface based on donor-acceptor interactions between the  $\pi$ -electrons of the heterocyclic nucleus and the empty d-orbital of the surface iron, but also adsorption can take place through the interaction between the free electron pairs of oxygen or other heteroatoms existing within the extract of the inhibitor and d-orbital vacant iron atoms on the surface.

### Conclusions

- The *OEE* shows a moderate efficiency in 1 N HCl, it increases when increasing the concentration of the extract.

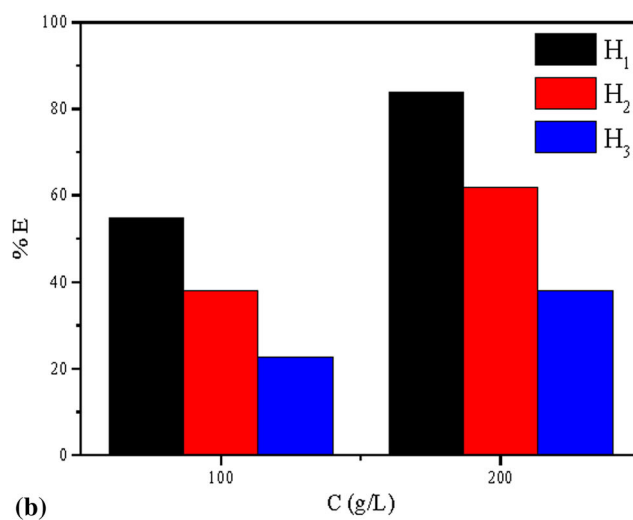


**Fig. 8** (a) Plot of corrosion rate as a function of the concentration of fractions H<sub>1</sub>, H<sub>2</sub> and H<sub>3</sub> (b) Inhibition efficiency as a function of fractions H<sub>1</sub>, H<sub>2</sub> and H<sub>3</sub> concentration

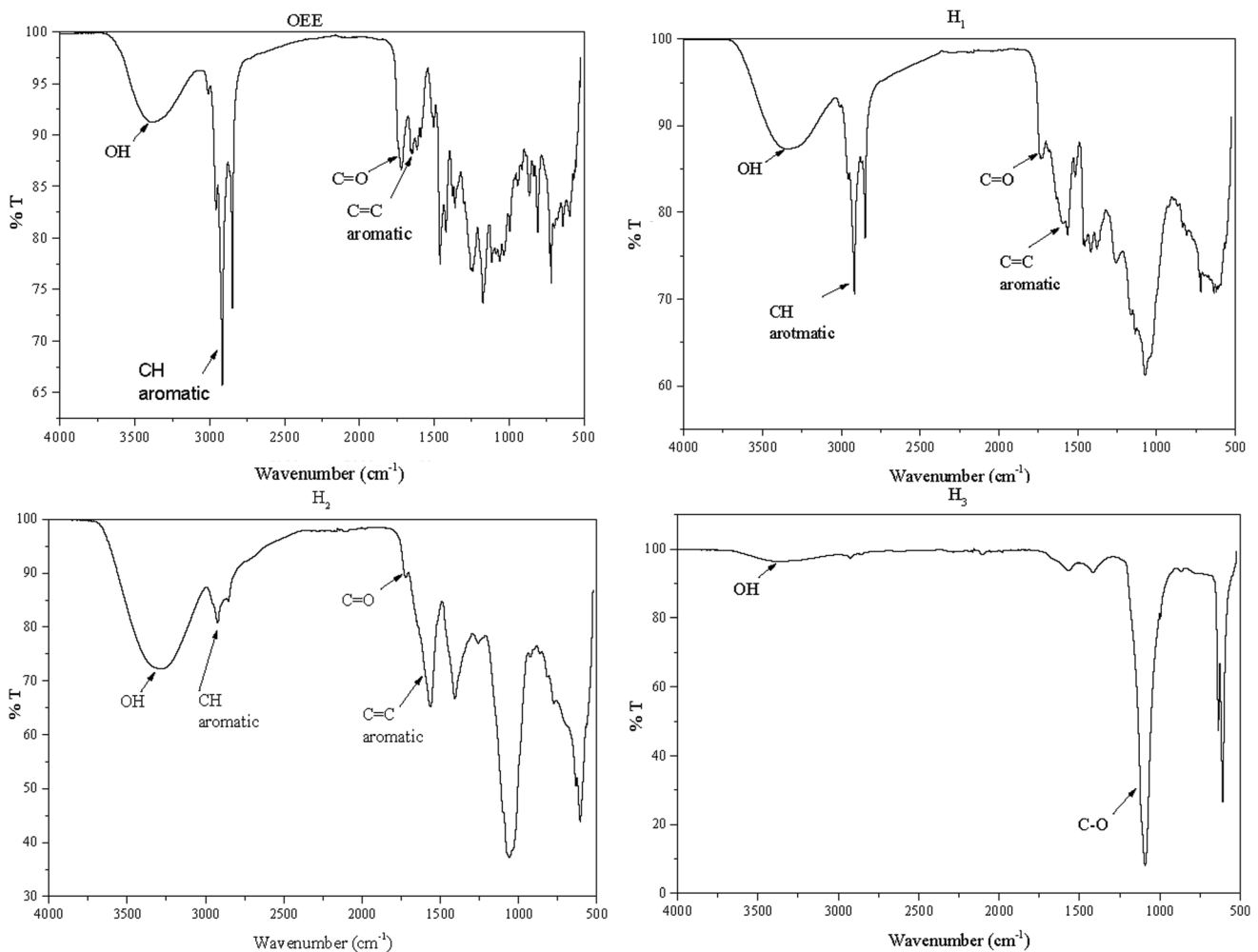


**Fig. 9** FTIR spectroscopy of the *OEE* and the different fractions  $H_1$ ,  $H_2$  and  $H_3$

- The linear polarization curves indicate that the extract blocks both types of reactions (anodic and cathodic), hence its nature as a mixed inhibitor.
- Impedance spectroscopy shows an increase in charge transfer resistance ( $R_{ct}$ ) and a decrease in double layer capacitance ( $C_{dl}$ ), which shows that the inhibition is by adsorption.
- The adsorption of the molecules of the extract on the metal surface obeys the modified Langmuir isotherm, the values of  $\Delta G_{ads}$  shows that it is a physisorption, while the value of  $\Delta H_{ads}$  shows that the adsorption of the molecules on the surface is an exothermic process.
- The fraction has led to three different fractions that represent efficiencies that decrease when the polarity decreases, this opens doors to search for or active molecules in the  $H_1$  fraction but also the polarity-corrosion inhibition relationship.
- We plan to redo the fractionation with solutions that are still selectively folded and focus on the first fraction to

find the molecule(s) responsible for the corrosion-inhibiting effect.

## References

1. D. Daoud, T. Douadi, S. Issaadi, S. Chafaa, Adsorption and corrosion inhibition of new synthesized thiophene Schiff base on mild steel X52 in HCl and H<sub>2</sub>SO<sub>4</sub> solutions. *Corros. Sci.* **79**, 50–58 (2014). <https://doi.org/10.1016/j.corsci.2013.10.025>
2. X. Li, X. Xie, S. Deng, G. Du, Inhibition effect of two mercaptoprimidine derivatives on cold rolled steel in HCl solution. *Corros. Sci.* **92**, 136–147 (2015). <https://doi.org/10.1016/j.corsci.2014.11.044>
3. M.A. Hegazy, A.S. El-tabei, A.H. Bedair, M.A. Sadeq, An investigation of three novel nonionic surfactants as corrosion inhibitor for carbon steel in 0.5 M H<sub>2</sub>SO<sub>4</sub>. *Corros. Sci.* **54**, 219–230 (2012). <https://doi.org/10.1016/j.corsci.2011.09.019>
4. F.E. Heakal, S.K. Attia, S.A. Rizk et al., Synthesis, characterization and computational chemical study of novel pyrazole derivatives as anticorrosion and antisclatant agents. *J. Mol. Struct.* **1147**, 714–724 (2017). <https://doi.org/10.1016/j.molstruc.2017.07.006>

5. C. Verma, M.A. Quraishi, A. Singh, 2-Amino-5-nitro-4,6-diarlylcyclohex-1-ene-1,3,3-tricarbonitriles as new and effective corrosion inhibitors for mild steel in 1 M HCl : experimental and theoretical studies. *J. Mol. Liq.* **212**, 804–812 (2015). <https://doi.org/10.1016/j.molliq.2015.10.026>
6. A. Reza, H. Zadeh, I. Danaee, M.H. Maddahy, Thermodynamic and Adsorption Behaviour of Medicinal Nitramine as a Corrosion Inhibitor for AISI Steel Alloy in HCl Solution. *J. Mater. Sci. Technol.* **29**, 884–892 (2013). <https://doi.org/10.1016/j.jmst.2013.06.006>
7. I.B. Obot, S.A. Umoren, Z.M. Gasem et al., Theoretical prediction and electrochemical evaluation of vinylimidazole and allylimidazole as corrosion inhibitors for mild steel in 1 M HCl. *J. Ind. Eng. Chem.* **21**, 1328–1339 (2015). <https://doi.org/10.1016/j.jiec.2014.05.049>
8. A. El Bribri, M. Tabyaoui, B. Tabyaoui et al., The use of Euphorbia falcata extract as eco-friendly corrosion inhibitor of carbon steel in hydrochloric acid solution. *Mater. Chem. Phys.* **141**, 240–247 (2013). <https://doi.org/10.1016/j.matchemphys.2013.05.006>
9. M. Boukklah, N. Benchat, B. Hammouti et al., Thermodynamic characterisation of steel corrosion and inhibitor adsorption of pyridazine compounds in 0.5 M H<sub>2</sub>SO<sub>4</sub>. *Mater. Lett.* **60**, 1901–1905 (2006). <https://doi.org/10.1016/j.matlet.2005.12.051>
10. E.M.S. Azzam, M.A. Hegazy, N.G. Kandil et al., The performance of hydrophobic and hydrophilic moieties in synthesized thiol cationic surfactants on corrosion inhibition of carbon steel in HCl. *Egypt. J. Pet.* **24**, 493–503 (2015). <https://doi.org/10.1016/j.ejpe.2015.02.012>
11. M.A. Amin, K.F. Khaled, Monitoring corrosion and corrosion control of iron in HCl by non-ionic surfactants of the TRITON-X series – Part I. Tafel polarisation ICP-AES and EFM Studies. *Corrosion Sci.* **52**, 1762–1770 (2010). <https://doi.org/10.1016/j.corsci.2009.12.033>
12. M. Lebrini, F. Robert, A. Lecante, C. Roos, Corrosion inhibition of C38 steel in 1M hydrochloric acid medium by alkaloids extract from Oxandra asbeckii plant. *Corros. Sci.* **53**, 687–695 (2011). <https://doi.org/10.1016/j.corsci.2010.10.006>
13. N. Soltani, N. Tavakkoli, M. Khayatkashani et al., Green approach to corrosion inhibition of 304 stainless steel in hydrochloric acid solution by the extract of Salvia officinalis leaves. *Corros. Sci.* **62**, 122–135 (2012). <https://doi.org/10.1016/j.corsci.2012.05.003>
14. L. Bammou, M. Belkhaouda, R. Salghi et al., Corrosion inhibition of steel in sulfuric acidic solution by the Chenopodium Ambrosioides Extracts. *J. Assoc. Arab Univ. Basic Appl. Sci.* (2013). <https://doi.org/10.1016/j.jaubas.2013.11.001>
15. P. Muthukrishnan, B. Jeyaprabha, P. Prakash, Adsorption and corrosion inhibiting behavior of Lannea coromandelica leaf extract on mild steel corrosion. *Arab. J. Chem.* **10**, S2343–S2354 (2017). <https://doi.org/10.1016/j.arabjc.2013.08.011>
16. J. Bhawsar, Experimental and computational studies of Nicotiana tabacum leaves extract as green corrosion inhibitor for mild steel in acidic medium. *Alex. Eng. J.* **54**, 769–775 (2015). <https://doi.org/10.1016/j.aej.2015.03.022>
17. M.H. Hussin, M.J. Kassim, N.N. Razali et al., The effect of Tinospora crispa extracts as a natural mild steel corrosion inhibitor in 1 M HCl solution. *Arab. J. Chem.* **9**, S616–S624 (2016). <https://doi.org/10.1016/j.arabjc.2011.07.002>
18. E.A. Noor, The impact of some factors on the inhibitory action of Radish seeds aqueous extract for mild steel corrosion in 1 M H<sub>2</sub>SO<sub>4</sub> solution. *Mater. Chem. Phys.* **131**, 160–169 (2011). <https://doi.org/10.1016/j.matchemphys.2011.08.001>
19. S.A. Umoren, M.M. Solomon, U.M. Eduok et al., Inhibition of mild steel corrosion in H<sub>2</sub>SO<sub>4</sub> solution by coconut coir dust extract obtained from different solvent systems and synergistic effect of iodide ions: ethanol and acetone extracts. *J. Environ. Chem. Eng.* (2014). <https://doi.org/10.1016/j.jece.2014.03.024>
20. A. Khadraoui, A. Khelifa, K. Hachama, R. Mehdaoui, Thymus algeriensis extract as a new eco-friendly corrosion inhibitor for 2024 aluminium alloy in 1 M HCl medium. *J. Mol. Liq.* (2015). <https://doi.org/10.1016/j.molliq.2015.12.064>
21. M. Sangeetha, S. Rajendran, J. Sathiyabama, A. Krishnaveni, Corrosion inhibition by an aqueous extract of phyllanthus amarus. *Port. Electrochim. Acta.* **29**, 429–444 (2011). <https://doi.org/10.4152/pea.201106429>
22. M. Fennane, M. Rejdali, Aromatic and medicinal plants of Morocco : Richness, diversity and threats Plantes aromatiques et médicinales du Maroc : Richesse, diversité et menaces. *Bulletin de l'Institut Scientifique, Rabat, Section Sciences de la Vie.* **38**, 27–42 (2016)
23. I. Tagnaout, H. Zerkan, S. Amine et al., Phenolic composition and antioxidant potential of different solvent extracts of the endemic Origanum elongatum (Bonnet) Emberger & Maire. *Mediterranean J. Chem.* **10**, 146–154 (2020)
24. H. Oualili, R. Nmila, F. Chibi et al., Chemical composition and antioxidant activity of origanum elongatum essential oil plant material. *Pharmacogn. Res.* **11**, 283–289 (2019). <https://doi.org/10.4103/pr.pr>
25. M.E. Belghiti, S. Bouazama, S. Echih et al., Understanding the adsorption of newly Benzylidene-aniline derivatives as a corrosion inhibitor for carbon steel in hydrochloric acid solution: Experimental, DFT and molecular dynamic simulation studies. *Arabian J. Chem.* (2017). <https://doi.org/10.1016/j.arabjc.2017.12.003>
26. H. Ramzi, M.R. Ismaili, M. Aberchane, S. Zaanoun, Chemical characterization and acaricidal activity of Thymus satureioides C. & B. and Origanum elongatum E. & M. (Lamiaceae) essential oils against Varroa destructor Anderson & Trueman (Acari: Varroidae). *Ind. Crops Prod.* **108**, 201–207 (2017). <https://doi.org/10.1016/j.indcrop.2017.06.031>
27. H. Elattari, K. Chefra, H. Rchid, R. Nmila, Corrosion inhibition study of the Origanum elongatum extract: electrochemical, gravimetric and adsorption isotherms studies in 05 M sulfuric acid. *Res. J. Pharmaceutic., Biol. Chem. Sci.* **1**, 1491 (2019)
28. M.A. Deyab, K. Eddahaoui, R. Essehli et al., Experimental evaluation of new inorganic phosphites as corrosion inhibitors for carbon steel in saline water from oil source wells. *Desalination.* **383**, 38–45 (2016). <https://doi.org/10.1016/j.desal.2016.01.019>
29. M. Yadav, L. Gope, N. Kumari, P. Yadav, Corrosion inhibition performance of pyranopyrazole derivatives for mild steel in HCl solution : gravimetric, electrochemical and DFT studies. *J. Mol. Liq.* **216**, 78–86 (2016). <https://doi.org/10.1016/j.molliq.2015.12.106>
30. A. Dehghani, G. Bahlakeh, B. Ramezanzadeh, M. Ramezanzadeh, A combined experimental and theoretical study of green corrosion inhibition of mild steel in HCl solution by aqueous Citrullus lanatus fruit (CLF) extract. *J. Mol. Liquids.* (2019). <https://doi.org/10.1016/j.molliq.2019.02.010>
31. D. Yang, Y. Ye, Y. Su et al., Functionalization of citric acid-based carbon dots by imidazole toward novel green corrosion inhibitor for carbon steel. *J. Clean. Prod.* **229**, 180–192 (2019). <https://doi.org/10.1016/j.jclepro.2019.05.030>
32. A. Bousskri, A. Anejjar, M. Messali et al., Corrosion inhibition of carbon steel in aggressive acidic media with 1- (2- (4-chlorophenyl ) -2-oxoethyl ) pyridazinium bromide. *J. Mol. Liq.* **211**, 1000–1008 (2015). <https://doi.org/10.1016/j.molliq.2015.08.038>
33. M. Faustini, A. Maciuk, P. Salvin et al., Corrosion inhibition of C38 steel by alkaloids extract of Geissosporium laeve in 1M hydrochloric acid: electrochemical and phytochemical studies. *Corros. Sci.* **92**, 287–300 (2015). <https://doi.org/10.1016/j.corsci.2014.12.005>

34. X. Li, S. Deng, H. Fu, Triazolyl blue tetrazolium bromide as a novel corrosion inhibitor for steel in HCl and H<sub>2</sub>SO<sub>4</sub> solutions. *Corros. Sci.* **53**, 302–309 (2011). <https://doi.org/10.1016/j.corsci.2010.09.036>
35. X. Li, S. Deng, H. Fu, Adsorption and inhibition effect of vanillin on cold rolled steel in 3.0 M H<sub>3</sub>PO<sub>4</sub>. *Prog. Org. Coat.* **67**, 420–426 (2010). <https://doi.org/10.1016/j.porgcoat.2009.12.006>
36. K. Hanini, B. Merzoug, S. Boudiba et al., Influence of different polyphenol extracts of *Taxus baccata* on the corrosion process and their effect as additives in electrodeposition. *Sustain. Chem. Pharmacy.* **14**, 100189 (2019). <https://doi.org/10.1016/j.scp.2019.100189>
37. M. Sundaravadivelu, G. Karthik, G. Vengatesh, A comprehensive study of ondansetron hydrochloride drug as a green corrosion inhibitor for mild steel in 1 M HCl medium A comprehensive study of ondansetron hydrochloride drug as a green corrosion inhibitor for mild steel in 1 M HCl medium. *Egypt. J. Pet.* (2016). <https://doi.org/10.1016/j.ejpe.2016.10.011>
38. K.R.G. Bacca, N.F. Lopes, J.B. Marcolino et al., Performance of Quebracho extract as eco - friendly corrosion inhibitor for SAE 1010 steel in the oil field environment. *Mater. Corros.* (2019). <https://doi.org/10.1002/maco.201910963>
39. S.A. Umoren, I.B. Obot, A.U. Israel et al., Inhibition of mild steel corrosion in acidic medium using coconut coir dust extracted from water and methanol as solvents. *J. Ind. Eng. Chem.* (2014). <https://doi.org/10.1016/j.jiec.2013.12.056>
40. M. Benarioua, A. Mihi, N. Bouzeghaia, M. Naoun, Mild steel corrosion inhibition by Parsley (*Petroselinum Sativum*) extract in acidic media. *Egypt. J. Pet.* **28**, 155–159 (2019). <https://doi.org/10.1016/j.ejpe.2019.01.001>
41. A. Espinoza-vázquez, G.E. Negrón-silva, R. González-olvera, D. Angeles-beltrán, Mild steel corrosion inhibition in HCl by di-alkyl and di-1, 2, 3-triazole derivatives of uracil and thymine. *Mater. Chem. Phys.* **145**, 407–417 (2014). <https://doi.org/10.1016/j.matchemphys.2014.02.029>
42. C. Verma, M.A. Quraishi, 2-Amino-4-(2,4-dihydroxyphenyl)quinoline-3-carbonitrile as sustainable corrosion inhibitor for SAE 1006 steel in 1 M HCl: Electrochemical and surface investigation. *J. Assoc. Arab Univ. Basic Appl. Sci.* **23**, 29–36 (2017). <https://doi.org/10.1016/j.jaubas.2016.03.002>
43. A.Y. El-Etre, Inhibition of acid corrosion of carbon steel using aqueous extract of olive leaves. *J. Colloid Interface Sci.* **314**, 578–583 (2007). <https://doi.org/10.1016/j.jcis.2007.05.077>
44. T. Benabbouha, M. Siniti, A.H. El et al., Red algae haloptys incurvus extract as a green corrosion inhibitor of carbon steel in hydrochloric acid A. *J. Bio- and Tribo-Corros.* **4**, 1–12 (2018). <https://doi.org/10.1007/s40735-018-0161-0>
45. E. Ituen, O. Akaranta, A. James, S. Sun, Green and sustainable local biomaterials for oil field chemicals : *Griffonia simplicifolia* extract as steel corrosion inhibitor in hydrochloric acid. *Sustain. Mater. Technol.* **11**, 12–18 (2017). <https://doi.org/10.1016/j.susmat.2016.12.001>
46. H.H. Hassan, E. Abdelghani, M.A. Amin, Inhibition of mild steel corrosion in hydrochloric acid solution by triazole derivatives Part I Polarization and EIS studies. *Electrochim. Acta.* **52**, 6359–6366 (2007). <https://doi.org/10.1016/j.electacta.2007.04.046>
47. Q.B. Zhang, Y.X. Hua, Corrosion inhibition of mild steel by alkylimidazolium ionic liquids in hydrochloric acid. *Electrochim. Acta.* **54**, 1881–1887 (2009). <https://doi.org/10.1016/j.electacta.2008.10.025>
48. E. Ituen, O. Akaranta, A. James, Evaluation of performance of corrosion inhibitors using adsorption isotherm models : an overview. *Chem. Sci. Int. J.* **18**, 1–34 (2017). <https://doi.org/10.9734/CSIJ/2017/28976>
49. J.T. Nwabanne, V.N. Okafor, Adsorption and thermodynamics study of the inhibition of corrosion of mild steel in H<sub>2</sub>SO<sub>4</sub> medium using *vernonia amygdalina*. *J. Minerals Mater. Char. Eng.* **11**, 885–890 (2012). <https://doi.org/10.4236/jmmce.2012.119083>
50. A. Fathima, S. Abdul, S. Sethumanickam, Corrosion inhibition, adsorption and thermodynamic properties of poly ( vinyl alcohol-cysteine ) in molar HCl. *Arab. J. Chem.* **10**, S3358–S3366 (2014). <https://doi.org/10.1016/j.arabjc.2014.01.016>
51. Bruggen B Van der (2003) Freundlich Isotherm. *Encyclopedia of Membranes*
52. S. Sohn, D. Kim, Modification of Langmuir isotherm in solution systems—definition and utilization of concentration dependent factor. *Chemosphere.* **58**(58), 115–123 (2005). <https://doi.org/10.1016/j.chemosphere.2004.08.091>
53. R. Karthikaiselvi, S. Subhashini, Study of adsorption properties and inhibition of mild steel corrosion in hydrochloric acid media by water soluble composite poly ( vinyl alcohol- o - methoxy aniline ). *J. Assoc. Arab Univ. Basic Appl. Sci.* **16**, 74–82 (2014). <https://doi.org/10.1016/j.jaubas.2013.06.002>
54. S.S. Ae, S.M. Sayyah, M.M. El-Deeb et al., Adsorption and corrosion inhibitive properties of P(2-aminobenzothiazole) on mild steel in hydrochloric acid media. *Int. J. Industrial Chem.* **7**, 39–52 (2016). <https://doi.org/10.1007/s40090-015-0065-5>
55. N.O. Eddy, Theoretical and experimental studies on the corrosion inhibition potentials of some purines for aluminum in 0.1 M HCl. *J. Adv. Res.* **6**, 203–217 (2015). <https://doi.org/10.1016/j.jare.2014.01.004>
56. A.S. Fouda, A.A. Al-sarawy, F.S. Ahmed, H.M. El-abbasy, Corrosion inhibition of aluminum 6063 using some pharmaceutical compounds. *Corros. Sci.* **51**, 485–492 (2009). <https://doi.org/10.1016/j.corsci.2008.10.012>
57. T. Benabbouha, R. Nmila, M. Siniti et al., The brown algae *Cystoseira Baccata* extract as a friendly corrosion inhibitor on carbon steel in acidic media. *SN Appl. Sci.* **2**, 1–11 (2020). <https://doi.org/10.1007/s42452-020-2492-y>
58. D. Daoud, T. Douadi, H. Hamani et al., Corrosion inhibition of mild steel by two new S-heterocyclic compounds in 1 M HCl: experimental and computational study. *Corros. Sci.* **94**, 21–37 (2015). <https://doi.org/10.1016/j.corsci.2015.01.025>
59. M. Mobin, M. Basik, J. Aslam, Pineapple stem extract (Bromelain) as an environmental friendly novel corrosion inhibitor for low carbon steel in 1M HCl. *Measurement.* (2018). <https://doi.org/10.1016/j.measurement.2018.11.003>
60. H. El Attari, K. Lahmadi, A. El Bribri, M. Siniti, The adsorption and corrosion inhibition of some cationic gemini surfactants on carbon steel surface in hydrochloric acid. *Int. J. Mater. Chem.* **47**, 273–278 (2015). <https://doi.org/10.1016/j.corsci.2004.05.009>
61. S.M. Shaban, A.A. Abd-Elal, S.M. Tawfik, Gravimetric and electrochemical evaluation of three nonionic dithiol surfactants as corrosion inhibitors for mild steel in 1 M HCl solution. *J. Mol. Liq.* **216**, 392–400 (2016). <https://doi.org/10.1016/j.molliq.2016.01.048>
62. A. Saxena, D. Prasad, R. Haldhar, Investigation of corrosion inhibition effect and adsorption activities of *Achyranthes aspera* extract for mild steel in 0.5 M H<sub>2</sub>SO<sub>4</sub>. *J. Failure Anal. Prevent.* (2018). <https://doi.org/10.1007/s11668-018-0491-8>
63. A.Y. Musa, A.A.H. Kadhum, A.B. Mohamad et al., Inhibition of aluminum corrosion by phthalazinone and synergistic effect of halide ion in 1.0 M HCl. *Current Appl. Phys. J.* **12**, 325–330 (2012). <https://doi.org/10.1016/j.cap.2011.07.001>
64. N. Devi, S. Jagadeesan, K. Ayyasamy et al., Adsorption characteristics of Iota-carrageenan and Inulin biopolymers as potential corrosion inhibitors at mild steel/sulphuric acid interface. *J. Mol. Liq.* **232**, 9–19 (2017). <https://doi.org/10.1016/j.molliq.2017.02.054>
65. M. Yadav, R.R. Sinha, T.K. Sarkar et al., Application of new isonicotinamides as a corrosion inhibitor on mild steel in acidic

- medium : Electrochemical, SEM, EDX, AFM and DFT investigations. *J. Mol. Liq.* **212**, 686–698 (2015). <https://doi.org/10.1016/j.molliq.2015.09.047>
66. A. Khadiri, R. Saddik, K. Bekkouche et al., Gravimetric, electrochemical and quantum chemical studies of some pyridazine derivatives as corrosion inhibitors for mild steel in 1M HCl solution. *J. Taiwan Inst. Chem. Eng.* **58**, 552–564 (2015). <https://doi.org/10.1016/j.jtice.2015.06.031>
67. H.J. Al-Tameme, I.H. Hameed, S.A. Idan, M.Y. Hadi, Biochemical analysis of *Origanum vulgare* seeds by fourier-transform infrared (FT-IR) spectroscopy and gas chromatography-mass spectrometry (GC-MS). *J. Pharmacognosy Phytotherap.* **7**, 222–237 (2015). <https://doi.org/10.5897/JPP2015.0362>

**Publisher's Note** Springer Nature remains neutral with regard to jurisdictional claims in published maps and institutional affiliations.